



The Implications of High Black Hole Spins for the Origin of Binary Black Hole Mergers

A. Olejak and K. Belczynski

Nicolaus Copernicus Astronomical Center, Polish Academy of Sciences, ul. Bartycka 18, 00-716 Warsaw, Poland; aleksandra.olejak@wp.pl, chrisbelczynski@gmail.com

Received 2021 September 22; revised 2021 October 12; accepted 2021 October 12; published 2021 October 26

Abstract

The LIGO–Virgo collaboration has reported 50 black hole–black hole (BH–BH) mergers and 8 candidates recovered from digging deeper into the detector noise. The majority of these mergers have low effective spins pointing toward low BH spins and efficient angular momentum (AM) transport in massive stars as proposed by several models (e.g., the Tayler–Spruit dynamo). However, out of these 58 mergers, 7 are consistent with having high effective-spin parameter ($\chi_{\text{eff}} > 0.3$). Additionally, two events seem to have high effective spins sourced from the spin of the primary (more massive) BH. These particular observations could be used to discriminate between the isolated binary and dynamical formation channels. It might seem that high BH spins point to a dynamical origin if AM in stars is efficient and forms low-spinning BHs. In such a case dynamical formation is required to produce second and third generations of BH–BH mergers with typically high spinning BHs. Here we show, however, that isolated binary BH–BH formation naturally reproduces such highly spinning BHs. Our models start with efficient AM in massive stars that is needed to reproduce the majority of BH–BH mergers with low effective spins. Later, some of the binaries are subject to a tidal spin-up allowing the formation of a moderate fraction ($\sim 10\%$) of BH–BH mergers with high effective spins ($\chi_{\text{eff}} \gtrsim 0.4\text{--}0.5$). In addition, isolated binary evolution can produce a small fraction of BH–BH mergers with almost maximally spinning primary BHs. Therefore, the formation scenario of these atypical BH–BH mergers remains to be found.

Unified Astronomy Thesaurus concepts: [Black holes \(162\)](#); [Compact objects \(288\)](#); [Massive stars \(732\)](#)

1. Introduction

The LIGO–Virgo collaboration has announced detection of gravitational waves from ~ 50 double black hole (BH–BH) mergers (Abbott et al. 2019a, 2019b, 2021a; Fishbach & Holz 2020). An additional eight BH–BH merger candidates have been recently reported (Abbott et al. 2021b). The majority of all these events have low effective spins parameters: $\chi_{\text{eff}} = \frac{m_1 a_1 \cos \theta_1 + m_2 a_2 \cos \theta_2}{m_1 + m_2} \approx 0$, where m_i are BH masses, $a_i = cJ_i/Gm_i^2$ are dimensionless BH spin magnitudes (J_i being the BH angular momentum (AM), c the speed of light, G the gravitational constant), and θ_i are angles between the individual BH spins and the system orbital AM.

However, among the detections there are also several BH–BH mergers that are characterized by higher (nonzero) positive effective spins. In Table 1 we list the parameters of the five BH–BH mergers with the highest effective spins reported by Abbott et al. (2021a) with an additional two high effective-spin systems reported by Abbott et al. (2021b).

The formation of close BH–BH systems is an open issue with several formation channels proposed and discussed in the context of the LIGO–Virgo mergers. The major formation scenarios include the isolated binary evolution (Bond & Carr 1984; Tutukov & Yungelson 1993; Lipunov et al. 1997; Voss & Tauris 2003; Belczynski et al. 2010b; Dominik et al. 2012; Kinugawa et al. 2014; Belczynski et al. 2016a; de Mink & Mandel 2016; Eldridge & Stanway 2016; Hartwig et al. 2016; Mandel & de Mink 2016; Marchant et al. 2016; Spera et al. 2016; Woosley 2016; van den Heuvel et al. 2017;

Stevenson et al. 2017; Hainich et al. 2018; Kruckow et al. 2018; Marchant et al. 2019; Neijssel et al. 2019; Spera et al. 2019; Bavera et al. 2020, 2021; du Buisson et al. 2020; Qin et al. 2021), the dense stellar system dynamical channel (Portegies Zwart & McMillan 2000; Miller & Hamilton 2002a, 2002b; Gültekin et al. 2004, 2006; Portegies Zwart et al. 2004; O’Leary et al. 2007; Sadowski et al. 2008; Downing et al. 2010; Antonini & Perets 2012; Benacquista & Downing 2013; Bae et al. 2014; Mennekens & Vanbeveren 2014; Chatterjee et al. 2017; Hurley et al. 2016; Mapelli 2016; Rodriguez et al. 2016, 2018; VanLandingham et al. 2016; Arca-Sedda & Capuzzo-Dolcetta 2019; Askar et al. 2017; Banerjee 2018; Morawski et al. 2018; Samsing 2018; Di Carlo et al. 2019; Perna et al. 2019; Zevin et al. 2019; Kremer et al. 2020), isolated multiple (triple, quadruple) systems (Antonini et al. 2017; Silsbee & Tremaine 2017; Arca-Sedda et al. 2021; Liu & Lai 2018; Fragione & Kocsis 2019), mergers of binaries in galactic nuclei (Antonini & Perets 2012; Hamers et al. 2018; Hoang et al. 2018; Fragione et al. 2019), and primordial BH formation (Sasaki et al. 2016; Clesse & García-Bellido 2017; Green 2017; Carr & Silk 2018; De Luca et al. 2021).

BH spins and their orientations can play an important role in distinguishing between various BH–BH formation models. If the BH spins are not small, then their orientation may possibly distinguish between a binary evolution origin (predominantly aligned spins) and dynamical formation channels (more or less isotropic distribution of spin orientations). If the BHs formed out of stars have small spins (Spruit 2002; Hotokezaka & Piran 2017; Zaldarriaga et al. 2018; Fuller et al. 2019; Qin et al. 2019; Bavera et al. 2020; Belczynski et al. 2020; Olejak et al. 2020) then BH–BH mergers with high effective spins may challenge their isolated evolution origin. In dense stellar clusters, BHs may merge several times easily producing BHs with high spins and making a dynamical channel a prime site

Table 1
BH–BH Mergers with High Effective Spins

No.	Name ^a	χ_{eff}	m_1	m_2	a_1
1	GW190517	$0.52_{-0.19}^{+0.19}$	$37.4_{-7.6}^{+11.7}$	$25.3_{-7.3}^{+7.0}$...
2	GW170729	$0.37_{-0.25}^{+0.21}$	$50.2_{-10.2}^{+16.2}$	$34.0_{-10.1}^{+9.1}$...
3	GW190620	$0.33_{-0.25}^{+0.22}$	$57.1_{-12.7}^{+16.0}$	$35.5_{-12.3}^{+12.2}$...
4	GW190519	$0.31_{-0.22}^{+0.20}$	$66.0_{-12.0}^{+10.7}$	$40.5_{-11.1}^{+11.0}$...
5	GW190706	$0.28_{-0.29}^{+0.26}$	$67.0_{-13.3}^{+14.6}$	$38.2_{-13.3}^{+14.6}$...
6	GW190403	$0.70_{-0.27}^{+0.15}$	$88.0_{-32.9}^{+28.2}$	$22.1_{-9.0}^{+23.8}$	$0.92_{-0.22}^{+0.07}$
7	GW190805	$0.35_{-0.36}^{+0.30}$	$48.2_{-12.5}^{+17.5}$	$32.0_{-11.4}^{+13.4}$	$0.74_{-0.60}^{+0.22}$

Note.

^a Names are abbreviated. We include candidate detections as full astrophysical events. Parameters of the first five events are from original LIGO–Virgo analysis (Abbott et al. 2021a), while the remaining two are from deeper searches into the detector noise (Abbott et al. 2021b).

for such events (Fishbach et al. 2017; Gerosa & Berti 2017). However, the assumption about the BH natal spin (and the AM transport efficiency) also plays a role in the effective-spin distribution for the dynamical channel (Banerjee 2021).

In this study we show that the current understanding of stellar/binary astrophysics (Belczynski et al. 2021) and the degeneracy between the different formation channels do not allow for such a simple test of the origin of the LIGO–Virgo BH–BH mergers. To demonstrate this we show that although the isolated binary evolution channel produces mostly BH–BH mergers with low effective spins, a small but significant fraction of mergers is expected to have moderate or even high effective spins. Despite the assumption that stars slow down their rotation due to efficient AM transport, we find that tidal interactions are capable of spinning up some stars allowing formation of rapidly spinning BHs (Detmers et al. 2008; Kushnir et al. 2017; Qin et al. 2018).

2. Method

We use the population synthesis code *StarTrack* (Belczynski et al. 2002, 2008) with a model of star formation rates and metallicity distribution based on Madau & Dickinson (2014) described in Belczynski et al. (2020). We employ the delayed core-collapse supernova (SN) engine for neutron star/BH mass calculation (Fryer et al. 2012), with weak mass loss from pulsation pair instability supernovae (Belczynski et al. 2016b). BH natal kicks are calculated from a Maxwellian distribution with $\sigma = 265 \text{ km s}^{-1}$ and decreased by fallback during core collapse; this makes a significant fraction of BHs form without a natal kick (Mirabel & Rodrigues 2003). We assume our standard wind losses for massive O/B stars (Vink et al. 2001) and Luminous Blue Variable (LBV) winds (specific prescriptions for these winds are listed in Section 2.2 of Belczynski et al. 2010a). BH natal spins are calculated under the assumption that AM in massive stars is transported by the Tayler–Spruit magnetic dynamo (Spruit 2002) as adopted in the MESA stellar evolutionary code (Paxton et al. 2015). Such BH natal spins take values in the range $a \in 0.05\text{--}0.15$ (see Belczynski et al. 2020). Note that the modified classic Tayler–Spruit dynamo with a different nonlinear saturation mechanism of the Tayler instability (Fuller & Ma 2019; Fuller et al. 2019) causes larger magnetic field amplitudes, more efficient AM transport, and even lower final natal spins ($a \sim 0.01$). BH spin

may be increased if the immediate BH progenitors (Wolf–Rayet, WR) stars in close binaries are subject to tidal spin-up. In our calculations for BH–WR, WR–BH, and WR–WR binary systems with orbital periods in the range $P_{\text{orb}} = 0.1\text{--}1.3$ days the BH natal spin magnitude is fit from WR star spun-up MESA models (see Equation 15 of Belczynski et al. 2020), while for systems with $P_{\text{orb}} < 0.1$ day the BH spin is taken to be equal to $a = 1$. BH spins may also be increased by accretion in binary systems. We treat accretion onto a compact object during Roche-lobe overflow (RLOF) and from stellar winds using the analytic approximations presented in King et al. (2001) and Mondal et al. (2020). In the adopted approach the accumulation of matter on a BH is very inefficient so accretion does not noticeably affect the final BH spin. However, note that, e.g., Van Son et al. (2020) or Bavera et al. (2021) tested different super-Eddington accretion prescriptions finding that some BHs may be significantly spun up by accretion.

For common-envelope (CE) evolution we assume a 100% ($\alpha_{\text{CE}} = 1$) orbital energy transfer for CE ejection and we adopt 5% Bondi accretion rate onto the BHs during CE (Ricker & Taam 2008; MacLeod & Ramirez-Ruiz 2015; MacLeod et al. 2017). During the stable RLOF (whether it is a thermal- or nuclear-timescale mass transfer, TTMT/NTMT) we adopt the following input physics. If an accretor is a compact object (neutron star or BH) we allow for super-Eddington accretion with excess transferred mass lost with an AM specific to the accretor (Mondal et al. 2020). In all other cases, we allow a fraction of the transferred mass of $f_a = 0.5$ to be lost from the binary with a specific AM of the binary orbit $j_{\text{loss}} = 1.0$ (expressed in units of $2\pi A^2/P_{\text{orb}}$, A being an orbital separation; see Equation (33) of Belczynski et al. 2008).

RLOF stability is an important issue in the context of BH–BH system formation in the framework of the isolated binary evolution (Neijssel et al. 2019; Belczynski et al. 2021; Gallegos-Garcia et al. 2021; Marchant et al. 2021; Olejak et al. 2021). In the standard *StarTrack* evolution we impose rather liberal limits for CE (dynamical-timescale RLOF) to develop (see Belczynski et al. 2008): binaries with a donor star more massive than 2–3 times the mass of the accretor are subject to CE. In this model (for simplicity tagged here as CE model) the vast majority of BH–BH mergers form through CE evolution, although we find some cases ($\lesssim 1\%$) of BH–BH merger formation without any CE event. In the alternative model (non-CE model; detailed description in Olejak et al. 2021) we allow CE to be suppressed for some systems even with a mass ratio as high as 6–8 (Pavlovskii et al. 2017). In this model the majority of the BH–BH mergers form without any CE event (the orbital decrease is obtained through angular momentum loss during stable RLOF), although some ($< 10\%$) BH–BH mergers form with the assistance of CE.

For each model we calculate the evolution of 64 million massive, Population I/II binary systems. We use the star formation history and chemical evolution of the universe to obtain the BH–BH merger properties within an approximate reach of LIGO–Virgo (redshift $z < 1$). We use the same method as described in Belczynski et al. (2020).

3. Results

Figure 1 shows a typical example of binary system evolution without a CE phase leading to the formation of a BH–BH merger with a tidally spun-up primary BH (restricted RLOF stability criteria; Olejak et al. 2021). The rather unequal-mass

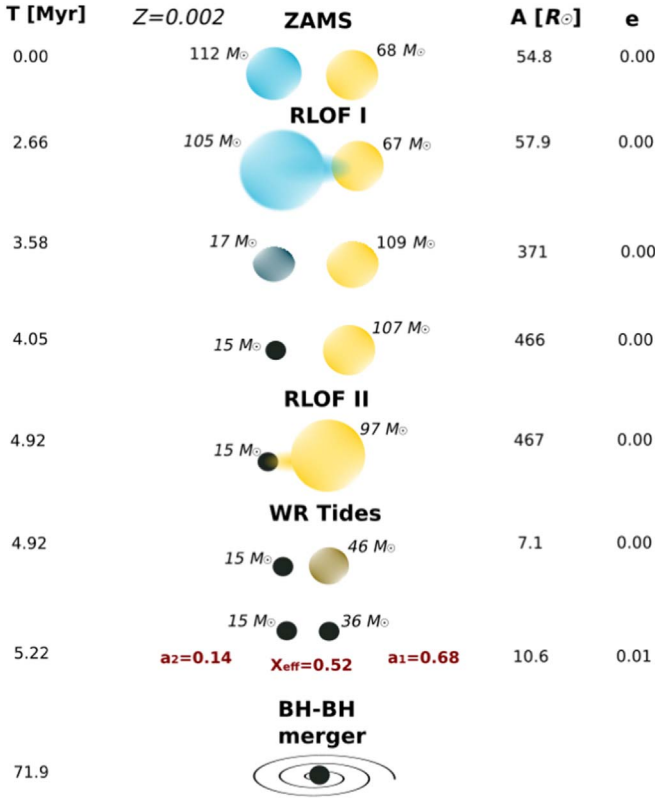


Figure 1. Typical example of a non-CE evolutionary scenario leading to the formation of a BH–BH merger with a tidally spun-up primary: $a_1 = 0.68$ and $\chi_{\text{eff}} = 0.52$. The binary system goes through two phases of RLOF with episodes of nuclear- and thermal-timescale mass transfer. RLOF I ends with the system mass ratio reversal. After RLOF II the system orbital separation significantly decreases and the WR star is a subject to tidal spin-up by a BH. Soon thereafter the close BH–BH system is formed with a short merger time of ~ 67 Myr (see Section 3).

massive stellar system ($112 M_{\odot}$ and $68 M_{\odot}$) with a metallicity of $Z = 0.002$ goes through two RLOF events. RLOF I is initiated by the more massive star; first by an NTMT when the donor is still on the main sequence and then through a TTMT when the donor evolves off the main sequence. After RLOF I, the system mass ratio is reversed: the initially more massive star lost over 80% of its mass while the companion gained $\sim 40 M_{\odot}$. Next, the initially more massive star ends its evolution directly collapsing to the less massive (secondary) BH with a mass of $m_2 = 15 M_{\odot}$ and spin $a_2 = 0.14$. When the companion star expands, it initiates a second stable RLOF. At the onset of RLOF II the system has highly unequal masses: the donor is almost 6.5 times more massive than the BH. The thermal timescale for a donor with mass $M_{\text{don}} \approx 97 M_{\odot}$, radius $R_{\text{don}} \approx 300 R_{\odot}$, and luminosity $L_{\text{don}} \approx 3 \times 10^6 L_{\odot}$ (parameters at the RLOF II onset¹) calculated with the formula by Kalogera & Webbink (1996) is $\tau_{\text{th}} \approx 330$ yr. It corresponds to a very high mass transfer rate $\dot{M} = M_{\text{don}}/\tau_{\text{th}} \approx 0.3 M_{\odot} \text{ yr}^{-1}$ that does not allow the BH to accrete much mass (despite the fact that we allow for super-Eddington accretion). Half of the donor’s mass is lost from the binary with the specific AM of the BH (as the matter was transferred to the vicinity of the BH accretor). This has a huge effect on the orbital separation that decreases from $A = 467 R_{\odot}$ to only $A = 7.1 R_{\odot}$. After RLOF II the binary

¹ Such parameter values are in line with other predictions for massive stars, e.g., using Geneva stellar evolution code (Yusof et al. 2013).

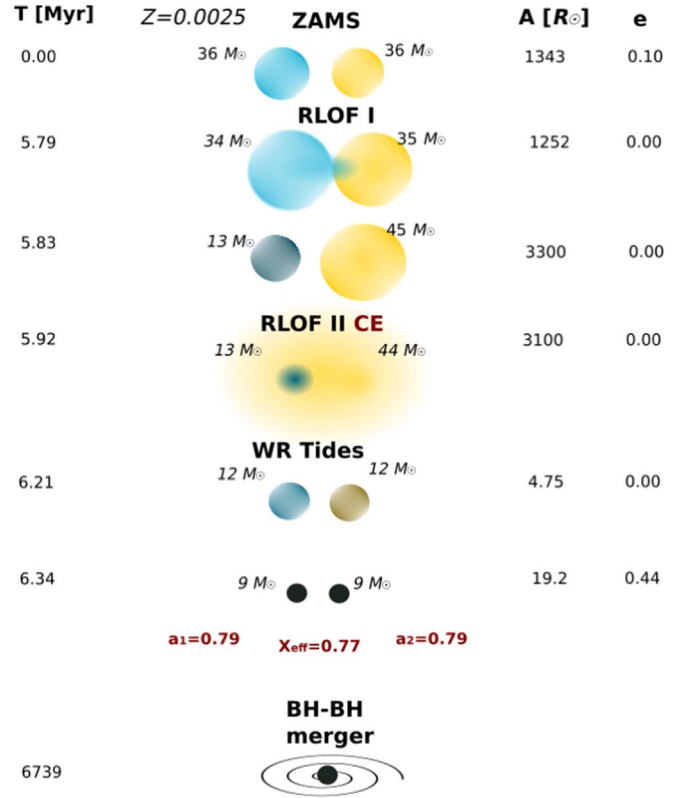


Figure 2. Typical example of an evolutionary scenario with the CE phase leading to the formation of a BH–BH merger with $a_1 = 0.79$, $a_2 = 0.79$, and $\chi_{\text{eff}} = 0.77$. First, the binary system goes through a stable RLOF phase with episodes of nuclear- and thermal-timescale mass transfer initiated by the initially more massive star. Then initially less massive star expands and initiates CE, after which the orbital separation is significantly decreased. After CE, the binary hosts two compact WR stars that are subject to tidal spin-up. Both stars explode as supernovae and form BHs on an eccentric orbit with a merger time of ~ 6.7 Gyr (see Section 3).

consists of a BH and a WR star that are close enough to allow for the tidal spin-up of the WR star. Finally, the WR star directly collapses to the more massive (primary) BH with a mass $m_1 = 36 M_{\odot}$ and spin $a_1 = 0.68$. The BH–BH system merges after ~ 67 Myr.

Figure 2 shows a typical CE evolution scenario (standard StarTrack RLOF stability criteria) leading to the formation of a BH–BH merger with both BHs spun up by tidal interactions. At the beginning, the binary system of two $\sim 36 M_{\odot}$ stars with $Z = 0.0025$ is on a wide ($A \approx 1340 R_{\odot}$) and eccentric ($e = 0.1$) orbit. When the initially more massive star expands the system goes through a stable RLOF, after which the donor loses its H-rich envelope and the orbit circularizes. Soon after RLOF I, the system goes through another (unstable) RLOF initiated by the initially less massive companion star. The ensuing CE evolution leads to significant orbital contraction from $A = 3100 R_{\odot}$ to $A = 4.5 R_{\odot}$ and leaves two WR stars subject to strong tidal interactions. Both stars end their evolution at a similar time forming via supernovae explosions two $\sim 9 M_{\odot}$ BHs. At the formation, both BHs get significant natal kicks that make the system orbit larger $A \approx 19 R_{\odot}$ and eccentric $e = 0.44$, leading to a merger time of ~ 6.7 Gyr.

In Table 2 we present the statistical spin properties of BH–BH systems merging at redshifts $z < 1$ for the two tested RLOF stability criteria models. In rows (1)–(6) we list the percentage of the BH–BH mergers with effective-spin parameter values

Table 2
Predictions for BH–BH Mergers from Binary Evolution

No.	Condition ^a	CE Model	Non-CE Model
1	$\chi_{\text{eff}} > 0.0$	97%	93%
2	$\chi_{\text{eff}} > 0.1$	95%	85%
3	$\chi_{\text{eff}} > 0.2$	70%	60%
4	$\chi_{\text{eff}} > 0.3$	36%	39%
5	$\chi_{\text{eff}} > 0.4$	10%	21%
6	$\chi_{\text{eff}} > 0.5$	2%	7%
7	$a_1 > 0.5$	3%	34%
8	$a_1 > 0.7$	2%	15%
9	$a_1 > 0.9$	1%	1%
10	$a_2 > 0.5$	52%	11%
11	$a_2 > 0.7$	33%	7%
12	$a_2 > 0.9$	12%	2%

Note.

^a We list fractions of BH–BH mergers (redshift $z < 1$) produced in our two population synthesis models satisfying a given condition.

$\chi_{\text{eff}} > 0.0, 0.1, 0.2, 0.3, 0.4,$ and 0.5 . In rows (7)–(9) we list the percentages of BH–BH mergers with a highly spinning primary BH $a_1 > 0.5, 0.7,$ and 0.9 while rows (10)–(12) give the percentages of mergers with a highly spinning secondary BH $a_2 > 0.5, 0.7,$ and 0.9 . The full distribution of the primary-spin, the secondary-spin, and the effective-spin parameters for both the CE and non-CE evolution is plotted in Figure 3 in the Appendix.

4. Discussion and Conclusions

The rapidly increasing number of detected BH–BH mergers allows for some general population statements (Abbott et al. 2021b; Galadage et al. 2021; Roulet et al. 2021). It appears that (i) the majority ($\sim 70\%$ – 90%) of BH–BH mergers have low effective spins consistent with $\chi_{\text{eff}} \approx 0$ and that (ii) a small fraction ($\sim 10\%$ – 30%) of mergers have positive nonzero spins that can be as high as $\chi_{\text{eff}} \gtrsim 0.5$. Additionally, the population is consistent with (iii) no systems having negative effective spins and (iv) a nonisotropic distribution of effective spins (which could indicate dynamical origin). Finally, (v) there is at least one case of a primary BH (more massive) in a BH–BH merger with very high spin ($a_1 > 0.7$ at 90% credibility). These properties are noted to be broadly consistent with BH–BH mergers being formed in an isolated binary evolution.

In our study we have tested whether we can reproduce the above spin characteristics with our binary evolution models that employ efficient AM transport in massive stars and that impose tidal spin-up of compact massive Wolf–Rayet stars in close binaries. The two presented models employ our standard input physics but allow for the formation of BH–BH mergers assisted either by a CE or by a stable RLOF. We find that the observed population and its spin characteristics (i)–(v) are consistent with our isolated-binary-evolution predictions (see Table 2). In particular, we find that the majority of BH–BH mergers have small positive effective spins: $\sim 70\%$ mergers have $0 < \chi_{\text{eff}} < 0.3$ (efficient AM transport), while a small fraction have significant spins: 36%–39% mergers have $\chi_{\text{eff}} > 0.3$ and 2%–7% mergers have $\chi_{\text{eff}} > 0.5$ (tidal spin-up). The fraction of systems with negative effective spins is small (3%–7%) as most BHs do not receive strong natal kicks in our simulations. Individual BH spins can reach high values. A large fraction (11%–52%) of secondary BHs may have

significant spin values ($a_2 > 0.5$) as it is the less massive stars that are most often subject to tidal spin-up. Nevertheless, primary BHs may also form with high spins (3%–34% with $a_1 > 0.5$) if both stars have similar masses and both are subject to tidal spin-up (see Figure 2) or due to mass ratio reversal caused by the RLOF (see Figure 1). We also note the formation of a small fraction of almost maximally spinning BHs: 2%–12% for $a_2 > 0.9$ (secondary BH) and 1% for $a_1 > 0.9$ (primary BH). These results on effective spins and individual BH spins are consistent with the current LIGO–Virgo population of BH–BH mergers. Note that Qin et al. (2021) came to different conclusions, finding the high spinning detections challenging for the Tayler–Spruit dynamo, especially for the unequal-mass event with a high spinning primary (GW190403). Our non-CE model reproduces this type of merger due to the mass ratio reversal (see Figure 1). In this channel, at the onset of the second stable RLOF, the donor may be even 5–6 times more massive than the accretor, ending as an unequal-mass ($q \leq 0.4$) BH–BH merger. Qin et al. (2021) have not considered the case of a stable RLOF in such unequal-mass systems.

The above fractions correspond to just two different modes of spinning up during the classical isolated binary BH–BH formation. Had we varied several other factors that influence BH spins and their orientations in BH–BH mergers, the ranges of these fractions would have broadened. Some obvious physical processes that can affect BH spins and their orientations include initial star spin alignment (or lack thereof) with the binary AM, the alignment of stellar spins (or lack thereof) during RLOF phases, the treatment of accretion, the initial mass ratio distribution that can alter the ratio of systems going through stable and unstable (CE) RLOF, and the natal kicks that can misalign spin orientations. Above all, the three major uncertainties include the initial stellar rotation of stars forming BHs, the efficiency of AM transport, and the strength of tides in close binary systems. All of the above are only weakly constrained. Note that this is a proof-of-principle study that is limited only to BH spins in BH–BH mergers. In particular, we did not try to match BH masses and BH–BH merger rates for the highly spinning LIGO–Virgo BHs. In this study we have only shown that it is possible to produce highly spinning BHs by tidal interactions of stars in close binaries in evolution that include and do not include CE. Our two examples of evolution (Figures 1 and 2) have much smaller masses than the LIGO–Virgo mergers with highly spinning BHs (Table 1). Note, however, that we have not used the input physics here that allows for the formation of BHs with mass over $50 M_{\odot}$. Such a model is already incorporated and tested within our population synthesis code (Belczynski 2020). An attempt to match all observed parameters simultaneously is projected to happen in the future when LIGO–Virgo will deliver a larger sample of highly spinning BHs.

Given the results presented in this study, alas limited only to BH spins, we conclude that (i) the isolated binary evolution channel reproduces well the BH spins of the LIGO–Virgo mergers; (ii) if, in fact, the binary channel is producing the majority of the LIGO–Virgo BH–BH mergers, then this indicates that the AM transport is efficient in massive stars and the tidal interactions in close binaries are strong.

We thank the anonymous reviewer, Jean-Pierre Lasota, Ilya Mandel, and Sambaran Banerjee for their useful comments on the manuscript. K.B. and A.O. acknowledge support from the

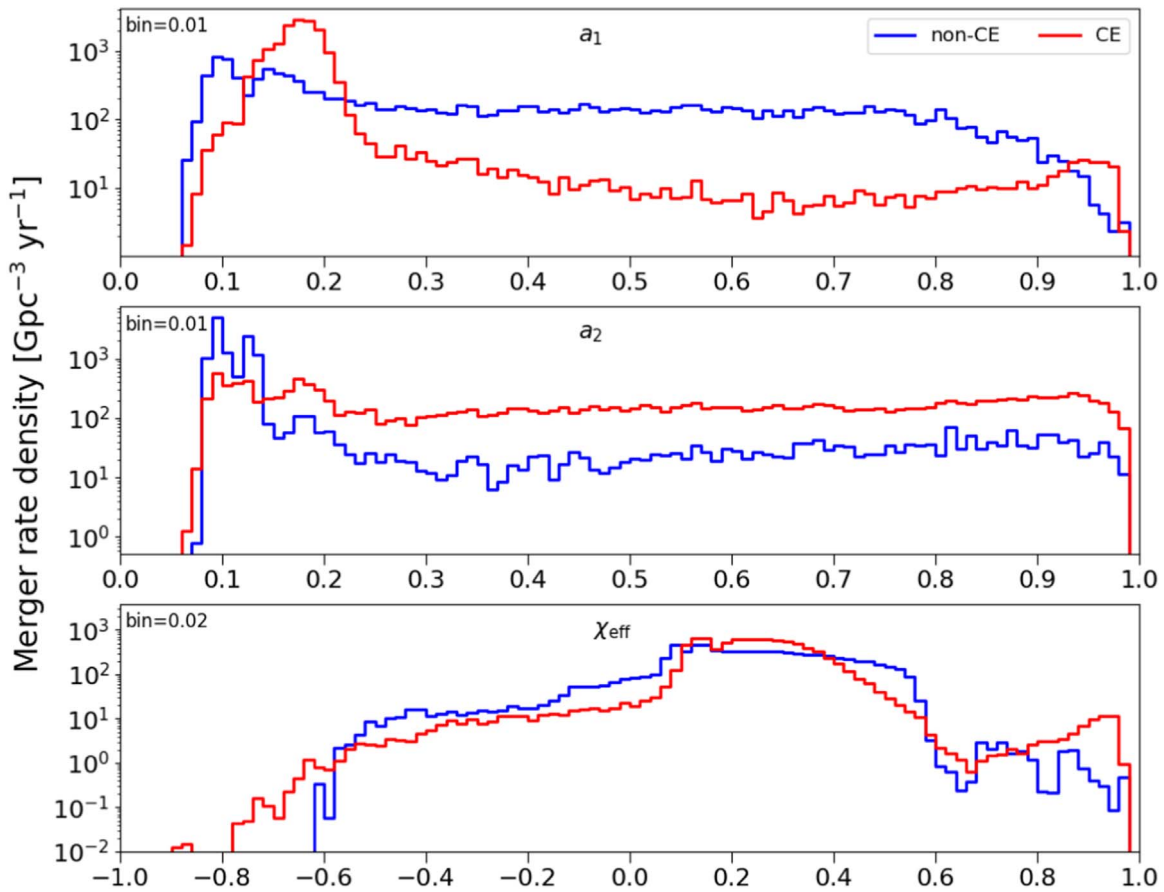


Figure 3. Distribution of (top panel) primary BH spin (a_1), (middle panel) secondary BH spin (a_2), and (bottom panel) effective-spin parameter (χ_{eff}) of BH–BH mergers at redshifts $z < 1.0$. The results are for two tested models: the non-CE model plotted with the red line, and the CE model plotted with the blue line. The figure is a supplement to the statistical spin predictions shown in Table 2 and described in Section 3.

Polish National Science Center (NCN) grant Maestro (2018/30/A/ST9/00050).

Appendix

In Figure 3 we plot the full distribution of the primary-spin, the secondary-spin and the effective-spin parameter for both the CE and non-CE evolution channels. The figure is a supplement to the statistical spin predictions shown in Table 2 and described in Section 3.

ORCID iDs

A. Olejak  <https://orcid.org/0000-0002-6105-6492>

References

- Abbott, B. P., Abbott, R., Abbott, T. D., et al. 2019a, *ApJL*, **882**, L24
 Abbott, B. P., Abbott, R., Abbott, T. D., et al. 2019b, *PhRvX*, **9**, 031040
 Abbott, R., Abbott, T. D., Abraham, S., et al. 2021a, *PhRvX*, **11**, 021053
 Abbott, R., Abbott, T. D., Acernese, F., et al. 2021b, arXiv:2108.01045
 Antonini, F., & Perets, H. B. 2012, *ApJ*, **757**, 27
 Antonini, F., Toonen, S., & Hamers, A. S. 2017, *ApJ*, **841**, 77
 Arca-Sedda, M., & Capuzzo-Dolcetta, R. 2019, *MNRAS*, **483**, 152
 Arca-Sedda, M., Li, G., & Kocsis, B. 2021, *A&A*, **650**, A189
 Askar, A., Szkudlarek, M., Gondek-Rosińska, D., Giersz, M., & Bulik, T. 2017, *MNRAS*, **464**, L36
 Bae, Y.-B., Kim, C., & Lee, H. M. 2014, *MNRAS*, **440**, 2714
 Banerjee, S. 2018, *MNRAS*, **473**, 909
 Banerjee, S. 2021, *MNRAS*, **500**, 3002
 Bavera, S. S., Fragos, T., Qin, Y., et al. 2020, *A&A*, **635**, A97
 Bavera, S. S., Fragos, T., Zevin, M., et al. 2021, *A&A*, **647**, A153
 Belczynski, K. 2020, *ApJL*, **905**, L15
 Belczynski, K., Bulik, T., Fryer, C. L., et al. 2010a, *ApJ*, **714**, 1217
 Belczynski, K., Dominik, M., Bulik, T., et al. 2010b, *ApJL*, **715**, L138
 Belczynski, K., Heger, A., Gladysz, W., et al. 2016b, *A&A*, **594**, A97
 Belczynski, K., Holz, D. E., Bulik, T., & O’Shaughnessy, R. 2016a, *Natur*, **534**, 512
 Belczynski, K., Kalogera, V., & Bulik, T. 2002, *ApJ*, **572**, 407
 Belczynski, K., Kalogera, V., Rasio, F. A., et al. 2008, *ApJS*, **174**, 223
 Belczynski, K., Klencek, J., Fields, C. E., et al. 2020, *A&A*, **636**, A104
 Belczynski, K., Romagnolo, A., Olejak, A., et al. 2021, arXiv:2108.10885
 Benacquista, M. J., & Downing, J. M. B. 2013, *LRR*, **16**, 4
 Bond, J. R., & Carr, B. J. 1984, *MNRAS*, **207**, 585
 Carr, B., & Silk, J. 2018, *MNRAS*, **478**, 3756
 Chatterjee, S., Rodriguez, C. L., Kalogera, V., & Rasio, F. A. 2017, *ApJL*, **836**, L26
 Clesse, S., & García-Bellido, J. 2017, *PDU*, **15**, 142
 De Luca, V., Desjacques, V., Franciolini, G., Pani, P., & Riotto, A. 2021, *PhRvL*, **126**, 051101
 de Mink, S. E., & Mandel, I. 2016, *MNRAS*, **460**, 3545
 Detmers, R. G., Langer, N., Podsiadlowski, P., & Izzard, R. G. 2008, *A&A*, **484**, 831
 Di Carlo, U. N., Giacobbo, N., Mapelli, M., et al. 2019, *MNRAS*, **487**, 2947
 Dominik, M., Belczynski, K., Fryer, C., et al. 2012, *ApJ*, **759**, 52
 Downing, J. M. B., Benacquista, M. J., Giersz, M., & Spurzem, R. 2010, *MNRAS*, **407**, 1946
 du Buisson, L., Marchant, P., Podsiadlowski, P., et al. 2020, *MNRAS*, **499**, 5941
 Eldridge, J. J., & Stanway, E. R. 2016, *MNRAS*, **462**, 3302
 Fishbach, M., & Holz, D. E. 2020, *ApJL*, **891**, L27
 Fishbach, M., Holz, D. E., & Farr, B. 2017, *ApJL*, **840**, L24
 Fragione, G., Grishin, E., Leigh, N. W. C., Perets, H. B., & Perna, R. 2019, *MNRAS*, **488**, 47
 Fragione, G., & Kocsis, B. 2019, *MNRAS*, **486**, 4781
 Fryer, C. L., Belczynski, K., Wiktorowicz, G., et al. 2012, *ApJ*, **749**, 91

- Fuller, J., & Ma, L. 2019, *ApJL*, **881**, L1
- Fuller, J., Piro, A. L., & Jermyn, A. S. 2019, *MNRAS*, **485**, 3661
- Galadage, S., Talbot, C., Nagar, T., et al. 2021, arXiv:2109.02424
- Gallegos-Garcia, M., Berry, C. P. L., Marchant, P., & Kalogera, V. 2021, arXiv:2107.05702
- Gerosa, D., & Berti, E. 2017, *PhRvD*, **95**, 124046
- Green, A. M. 2017, *PhRvD*, **96**, 043020
- Gültekin, K., Miller, M. C., & Hamilton, D. P. 2004, *ApJ*, **616**, 221
- Gültekin, K., Miller, M. C., & Hamilton, D. P. 2006, *ApJ*, **640**, 156
- Hainich, R., Oskinova, L. M., Shenar, T., et al. 2018, *A&A*, **609**, A94
- Hamers, A. S., Bar-Or, B., Petrovich, C., & Antonini, F. 2018, *ApJ*, **865**, 2
- Hartwig, T., Volonteri, M., Bromm, V., et al. 2016, *MNRAS*, **460**, L74
- Hoang, B.-M., Naoz, S., Kocsis, B., Rasio, F. A., & Dosopoulou, F. 2018, *ApJ*, **856**, 140
- Hotokezaka, K., & Piran, T. 2017, *ApJ*, **842**, 111
- Hurley, J. R., Sippel, A. C., Tout, C. A., & Aarseth, S. J. 2016, *PASA*, **33**, e036
- Kalogera, V., & Webbink, R. F. 1996, *ApJ*, **458**, 301
- King, A. R., Davies, M. B., Ward, M. J., Fabbiano, G., & Elvis, M. 2001, *ApJL*, **552**, L109
- Kinugawa, T., Inayoshi, K., Hotokezaka, K., Nakauchi, D., & Nakamura, T. 2014, *MNRAS*, **442**, 2963
- Kremer, K., Ye, C. S., Rui, N. Z., et al. 2020, *ApJS*, **247**, 48
- Kruckow, M. U., Tauris, T. M., Langer, N., Kramer, M., & Izzard, R. G. 2018, *MNRAS*, **481**, 1908
- Kushnir, D., Zaldarriaga, M., Kollmeier, J. A., & Waldman, R. 2017, *MNRAS*, **467**, 2146
- Lipunov, V. M., Postnov, K. A., & Prokhorov, M. E. 1997, *AstL*, **23**, 492
- Liu, B., & Lai, D. 2018, *ApJ*, **863**, 68
- MacLeod, M., Antoni, A., Murguía-Berthier, A., Macias, P., & Ramirez-Ruiz, E. 2017, *ApJ*, **838**, 56
- MacLeod, M., & Ramirez-Ruiz, E. 2015, *ApJ*, **803**, 41
- Madau, P., & Dickinson, M. 2014, *ARA&A*, **52**, 415
- Mandel, I., & de Mink, S. E. 2016, *MNRAS*, **458**, 2634
- Mapelli, M. 2016, *MNRAS*, **459**, 3432
- Marchant, P., Langer, N., Podsiadlowski, P., Tauris, T. M., & Moriya, T. J. 2016, *A&A*, **588**, A50
- Marchant, P., Pappas, K. M. W., Gallegos-Garcia, M., et al. 2021, *A&A*, **650**, A107
- Marchant, P., Renzo, M., Farmer, R., et al. 2019, *ApJ*, **882**, 36
- Mennekens, N., & Vanbeveren, D. 2014, *A&A*, **564**, A134
- Miller, M. C., & Hamilton, D. P. 2002a, *MNRAS*, **330**, 232
- Miller, M. C., & Hamilton, D. P. 2002b, *ApJ*, **576**, 894
- Mirabel, I. F., & Rodrigues, I. 2003, *Sci*, **300**, 1119
- Mondal, S., Belczyński, K., Wiktorowicz, G., Lasota, J.-P., & King, A. R. 2020, *MNRAS*, **491**, 2747
- Morawski, J., Giersz, M., Askar, A., & Belczynski, K. 2018, *MNRAS*, **481**, 2168
- Neijssel, C. J., Vigna-Gómez, A., Stevenson, S., et al. 2019, *MNRAS*, **490**, 3740
- O’Leary, R. M., O’Shaughnessy, R., & Rasio, F. A. 2007, *PhRvD*, **76**, 061504
- Olejak, A., Belczynski, K., & Ivanova, N. 2021, *A&A*, **651**, A100
- Olejak, A., Fishbach, M., Belczynski, K., et al. 2020, *ApJL*, **901**, L39
- Pavlovskii, K., Ivanova, N., Belczynski, K., & Van, K. X. 2017, *MNRAS*, **465**, 2092
- Paxton, B., Marchant, P., Schwab, J., et al. 2015, *ApJS*, **220**, 15
- Perna, R., Wang, Y.-H., Farr, W. M., Leigh, N., & Cantiello, M. 2019, *ApJL*, **878**, L1
- Portegies Zwart, S. F., Baumgardt, H., Hut, P., Makino, J., & McMillan, S. L. W. 2004, *Natur*, **428**, 724
- Portegies Zwart, S. F., & McMillan, S. L. W. 2000, *ApJL*, **528**, L17
- Qin, Y., Fragos, T., Meynet, G., et al. 2018, *A&A*, **616**, A28
- Qin, Y., Marchant, P., Fragos, T., Meynet, G., & Kalogera, V. 2019, *ApJL*, **870**, L18
- Qin, Y., Wang, Y.-Z., Dong-Hong, et al. 2021, arXiv:2108.04821
- Ricker, P. M., & Taam, R. E. 2008, *ApJL*, **672**, L41
- Rodriguez, C. L., Amaro-Seoane, P., Chatterjee, S., et al. 2018, *PhRvD*, **98**, 123005
- Rodriguez, C. L., Haster, C.-J., Chatterjee, S., Kalogera, V., & Rasio, F. A. 2016, *ApJL*, **824**, L8
- Roulet, J., Chia, H. S., Olsen, S., et al. 2021, *PhRvD*, **104**, 083010
- Sadowski, A., Belczynski, K., Bulik, T., et al. 2008, *ApJ*, **676**, 1162
- Samsing, J. 2018, *PhRvD*, **97**, 103014
- Sasaki, M., Suyama, T., Tanaka, T., & Yokoyama, S. 2016, *PhRvL*, **117**, 061101
- Silber, K., & Tremaine, S. 2017, *ApJ*, **836**, 39
- Spera, M., Giacobbo, N., & Mapelli, M. 2016, *MmSAI*, **87**, 575
- Spera, M., Mapelli, M., Giacobbo, N., et al. 2019, *MNRAS*, **485**, 889
- Spruit, H. C. 2002, *A&A*, **381**, 923
- Stevenson, S., Vigna-Gómez, A., Mandel, I., et al. 2017, *NatCo*, **8**, 14906
- Tutukov, A. V., & Yungelson, L. R. 1993, *MNRAS*, **260**, 675
- van den Heuvel, E. P. J., Portegies Zwart, S. F., & de Mink, S. E. 2017, *MNRAS*, **471**, 4256
- Van Son, L. A. C., De Mink, S. E., Broekgaarden, F. S., et al. 2020, *ApJ*, **897**, 100
- VanLandingham, J. H., Miller, M. C., Hamilton, D. P., & Richardson, D. C. 2016, *ApJ*, **828**, 77
- Vink, J. S., de Koter, A., & Lamers, H. J. G. L. M. 2001, *A&A*, **369**, 574
- Voss, R., & Tauris, T. M. 2003, *MNRAS*, **342**, 1169
- Woosley, S. E. 2016, *ApJL*, **824**, L10
- Yusof, N., Hirschi, R., Meynet, G., et al. 2013, *MNRAS*, **433**, 1114
- Zaldarriaga, M., Kushnir, D., & Kollmeier, J. A. 2018, *MNRAS*, **473**, 4174
- Zevin, M., Samsing, J., Rodriguez, C., Haster, C.-J., & Ramirez-Ruiz, E. 2019, *ApJ*, **871**, 91